Life Sciences 232 (2019) 116618

Contents lists available at ScienceDirect

Life Sciences

journal homepage: www.elsevier.com/locate/lifescie

PD98059 protects the brain against mitochondrial-mediated apoptosis and autophagy in a cardiac arrest rat model

Jun-Hui Zheng[a,1], Lu Xie[b,1], Nuo Li[a], Zhao-Yin Fu[a], Xiao-Feng Tan[a], Ran Tao[a], Tao Qin[a], Meng-Hua Chen[a,*]

[a] Department of Intensive Care Unit, The Second Affiliated Hospital of Guangxi Medical University, Nanning, Guangxi 530000, China
[b] Department of Physiology, Pre-Clinical Science, Guangxi Medical University, Nanning, Guangxi 530021, China

ARTICLE INFO

Keywords:
Cardiopulmonary resuscitation
Extracellular signaling pathway
Apoptosis
Autophagy
Dynamin-related protein 1

ABSTRACT

Aims: Mitochondrial dysfunction has been regarded as one of the hallmarks of cerebral ischemia-reperfusion injury. In previous studies, we have provided evidence that the extracellular signaling pathway (ERK) 1/2 inhibitor PD98059 improved the neurological deficits by modulating antioxidant and anti-apoptotic activities in rats subjected to cardiac arrest/cardiopulmonary resuscitation (CA/CPR). Since oxidative stress can activate mitochondria-dependent apoptosis and autophagy, we further explored the effects of PD98059 on mitochondria involved with apoptosis and autophagy in rat CA model.

Materials and methods: We disposed PD98059 in CA/CPR rats, tested the mitochondrial-mediated apoptosis pathway in brain tissues at 24 h post-resuscitation by mitochondrial permeability transition pores (MPTP), cytochrome *c* (CytC), BCL-2, BAX, caspase-3, as well as autophagy by LC3, Beclin-1, and p62. Furthermore, we explored the relationship of dynamin-related protein 1 (Drp1) with apoptosis and autophagy.

Key findings: Our study showed that PD98059 decreased the openings of MPTP, CytC release, caspase3 activation, apoptotic indices, LC3-II, Beclin-1and increased P62. PD98059 also inhibited mitochondria-dependent apoptosis and the activity of autophagy in a dose-dependent manner in rat cerebral cortices at 24 h post-resuscitation. The generation of phosphorylated Drp1-616 was down-regulated accompanied by a decrease of TUNEL-positive cells and LC3 in dual immunostaining after PD98059 inhibited activation of ERK signaling pathway in a dose-dependent manner in rat cerebral cortices at 24 h post-resuscitation.

Significance: PD98059 protects the brain against mitochondrial-mediated apoptosis and autophagy at 24 h post-resuscitation in rats subjected to CA/CPR, which is linked with the downregulation of Drp1 expression.

1. Introduction

When cerebral ischemia occurs, the restoration of blood supply to the tissues can result in cerebral ischemia-reperfusion injury (CIRI) due to the high degree of oxidative stress [1–5]. Mitochondrial dysfunction has been regarded as one of the hallmarks of CIRI [6,7]. Mitochondrial damage plays essential roles in metabolic disorders, energy deficiencies, and cell death as apoptosis [8], autophagy [9], and necroptosis [10].

Apoptosis can be mediated by mitochondria-initiated intrinsic pathway. In cerebral ischemia-reperfusion (CIR), the opening of the mitochondrial permeability transition pores (MPTP) [11] result from the overproduction of free radicals. In return, high levels of cytochrome *c* (CytC) are released into the cytoplasm, which induces the expression of the apoptosis-associated enzyme known as caspase-3 [12]. Accumulated evidence has suggested that CIR may promote apoptotic cell death through a mitochondrial-dependent pathway [13,14]. This phenomenon was verified by Zhou et al. [15] and Wu et al. [16] in the brains of rats after cardiac arrest/cardiopulmonary (CA/CPR).

Autophagy is a natural mechanism of regeneration required for the maintenance of cellular homeostasis in humans. Several studies have shown direct correlations between autophagy levels and cell death in vitro and in vivo [17,18]. In addition, there is growing evidence supporting the notion that increased levels of reactive oxygen species (ROS) in damaged mitochondria after CIR can mediate the autophagy pathway [9]. Previously, Lu et al. [19] showed that autophagy could induce and promote the injury of nerve cells in a rat CA model.

The dysfunction of mitochondrial fission and fusion dynamics can

* Corresponding author at: The Second Affiliated Hospital of Guangxi Medical University, No.166 Daxuedong road,Nanning 530007 , China.
E-mail address: cmhnn@sina.com (M.-H. Chen).
[1] These authors contributed equally to this work.

https://doi.org/10.1016/j.lfs.2019.116618
Received 24 April 2019; Received in revised form 22 June 2019; Accepted 28 June 2019
Available online 29 June 2019

induce cellular stress and ultimately cell death [20,21]. Dynamin-related protein 1 (Drp1) is a cytosolic protein to interact with the outer membrane of mitochondria to regulate mitochondrial fission. The excessive activation Drp1 disrupts the homeostasis and functioning of the mitochondrial network, which leads to impaired mitochondrial function and cell stress. In addition, Drp1-mediated Bnip3-induced autophagy and its downregulation have been shown to suppress the formation of autophagosomes in response to glucose deprivation cardiomyocyte [20]. In previous studies, fission was found to be a necessary prerequisite for cellular apoptosis [21]. Hence, further research into the roles of mitochondrial injury and Drp1 dysfunction in apoptosis and autophagy may help physicians better assess and treat CIR patients in the clinic.

In our previous study, we showed that an ERK 1/2 inhibitor PD98059 could improve the neurological deficits in rats by promoting antioxidant activities and anti-apoptosis functions in a post-resuscitation global CIRI model [22]. However, the anti-apoptotic effect associated with the mitochondria-dependent pathway requires further investigation. Moreover, it is important to consider the strong relationship that exists between apoptosis and autophagy [23]. Therefore, in the current study, we further explored the effects of PD98059 on mitochondrial-dependent pathway apoptosis and autophagy. In addition, we investigated the relationship that Drp1 has with apoptosis and autophagy using a rat CA/CPR model. We determined the following indices of brain tissue: apoptosis-related MPTP, Cyt C, BCl-2, BAX, caspase-3, and TUNEL staining; autophagy-related protein LC3, Beclin-1, and p62 protein; Drp1-related apoptosis and autophagy showed by P-Drp/TUNEL and P-Drp/LC3 dual-staining.

2. Materials and methods

2.1. Animal preparation and animal grouping

Male Sprague-Dawley rats (210–270 g), aged 6 to 8 weeks, were purchased from the Experimental Animal Center of Guangxi Medical University (Nanning, P. R. China). The experimental protocol was approved by the Animal Ethics Committee of Guangxi Medical University. The experiments were also conducted in a manner that addressed the key elements of the ARRIVE Guidelines.

A total of 135 rats were randomly divided into five groups, including: (1) sham operation group (Sham, $n = 15$), the same procedure without CA/CPR in healthy rats; (2) Saline group (CA, $n = 30$), CA 6 min, femoral vein injection of saline after restoration of spontaneous circulation (ROSC); (3) Dimethylsulfoxide (DMSO) group (DMSO, $n = 30$), a control vehicle group, CA 6 min, femoral vein injection of 5% DMSO after ROSC; (4) PD98059 (PD0.15, $n = 30$), CA 6 min, femoral vein injection of 0.15 mg/kg PD98059 after ROSC; and (5) PD98059 group (PD0.3, n = 30), CA 6 min, femoral vein injection of 0.3 mg/kg PD98059 after ROSC.

2.2. Creation of the CA/CPR rat model

The CA model was created using methods described previously [24]. In brief, an alternating current of 12 V from a stimulator (Chengdu Technology & Market Co. Ltd., China) was sent through a pacing electrode located in the esophagus to induce CA. After 6 min of untreated CA, CPR was initiated. Manual Chest compressions (180 per minute) were controlled following the pace from a metronome, with a depth of 25%–30% of the anterior posterior diameter of the animal's chest and with equal compression-relaxation duration by the same investigator. Animals were orally intubated, followed by mechanical ventilation (DH-150, The Medical Instrument Department of Zhejiang University, China), a volume-controlled small animal ventilator, with room air at a rate of 70 strokes/min, a tidal volume of 6 ml/kg, and a positive end expiratory pressure (PEEP) of 0 cmH_2O. After 1 min of CPR, one dose of epinephrine (20 $mg{\cdot}kg^{-1}$) was given through the left femoral vein catheter. ROSC was defined as an organized cardiac rhythm with the mean aortic pressure of > 60 mmHg for ≥1 min. The rats were injected intravenously with saline, 5%DMSO, 0.15 mg/kg PD98059 or 0.3 mg/kg PD98059 within 1 min after ROSC. The resuscitation efforts were ceased when there was a failure to ROSC after 3 min of CPR. From anesthesia to awakening, the rat's rectal temperature was monitored continuously and maintained by a heating lamp at 37.0 ± 0.5 °C. After awakened completely, rats were returned to their cages with dry bedding and housed in an air-conditioned and peaceful room (room temperature 27 °C).

2.3. Survival observation and neurological evaluation

Survival rate and neurologic deficits were evaluated at 24 h post-resuscitation. Neurological deficit scores (NDS) were assessed using a method created by Jia et al. [25]. In brief, NDS includes the level of consciousness, exercise, sensory function, breathing pattern and behavior. Neurologic deficits were scored from 0 (death or brain death) to 80 (no observed neurologic deficit). Two independent investigators measured the NDS in the assessment and reached an agreement. The 15 rats in each group that survived were used for the subsequent immunoblotting and immunostaining tests to evaluate the occurrence of apoptosis and autophagy in the cerebral cortex.

2.4. Preparation of brain tissues

The 15 rats that survived were anesthetized using pentobarbital (60 mg/kg, i.p.) at 24 h post-reperfusion. The cerebral cortices of 4 rats in each group were detached for isolation of the mitochondria, while the cerebral cortices of the other 8 rats were immediately stored at −80 °C for immunoblotting and frozen sections. Three of the 15 surviving rats were perfused with 4% paraformaldehyde for tissue fixation to make tissue sections. The tissue sections were used for observing autophagy by electron microscopy, immunofluorescence and immunohistochemistry.

2.5. TUNEL staining and observation of autophagy by electron microscopy

Cell apoptosis was detected by fluorescence microscopy using the terminal deoxynucleotidyl transferase dUTP nick end labeling (TUNEL) assay kits (Hoffmann La Roche Ltd., Basel, Switzerland) based on the manufacturer's instructions. The percent of apoptotic cells was calculated as the ratio of TUNEL-positive cells divided by the number of total neurons using five fields of focus for each group.

We used a transmission electron microscope (TEM) to observe the autophagosomes formation at 24 h reperfusion in rat cortex following CA/CPR. 4% paraformaldehyde (pH 7.4, precooled to 4 °C) was perfused through left ventricle of the anesthetized rat heart, and a fraction of the left cerebral cortex layer was extracted and put it into 2.5% glutaraldehyde. The cortical area was fixed with 1% osmium tetroxide, and then dehydrated and embedded in epoxy resin. According to the standard principle of three-dimensional localization, 100 nm sections were randomly cut, mounted on a copper mesh, double stained with lead citrate and uranyl acetate, and then placed under TEM for observation morphology of the autophagosomes. Images were recorded and examined under an H-7650 TEM (Hitachi, Tokyo, Japan).

2.6. MPTP openings

Opened MPTPs were detected using an MPTP assay kit (Genmed Scientific, Inc., Shanghai, P. R. China) in mitochondria extracted from the tissue samples. Fluorescence intensity was measured using a monochromator microplate reader with an excitation of 488 nm and emission of 505 nm (Safire II, Tecan, Switzerland).

2.7. Western blot analysis

The protein was extracted from the brain tissues and mitochondria for western blot analysis. The protein lysates of 10–20 μl extracted from the brain tissues or mitochondria were separated on 10–15% sodium dodecyl sulfate-polyacrylamide gels by electrophoresis (SDS-PAGE) and transferred onto PVDF membranes. The PVDF was blocked with 5% bovine serum albumin for 1 h and incubated overnight at 4 °C with the corresponding primary antibodies. The primary antibodies were as follows: caspase-3 (CST, #9664), BCL-2 (ab194583), BAX (CST, #14796), CytC (CST, #11940), COX-IV (CST, #4850), LC3A/B (CST, #12741), Beclin-1 (CST, #3495), P62 (MBL, PM045), P-Drp (CST, #4494), Drp (CST, #8570), β-Actin (CST, #4970), GAPDH(ab181602), ERK1/2(ab184699) and P-ERK1/2 (ab76299).

2.8. Dual-immunofluorescence and immunohistochemical staining of tissues

Dual-staining for LC3 and TUNEL was detected using a fluorescence imaging strategy. After the slides were dewaxed, repaired, and sealed, the sections were incubated overnight at 4 °C with monoclonal antibodies against LC3 (1:50 dilution). Next, the sections were incubated with the secondary antibody (goat anti-rabbit IgG H&L Alexa Fluor 488, ab150079) and TUNEL reaction mix for 60 min at 37 °C.

Dual-staining for P-Drp and LC3 was detected using the fluorescence imaging strategy. Harvested brain samples were immediately frozen at −80 °C and cut using the CM1950 Cryostat Microtome (Leica, Windhagen, Germany). The sections were incubated with 10% normal goat serum at room temperature and the monoclonal antibodies against P-Drp (1:50 dilution) and LC3 (1:50 dilution) overnight at 4 °C. Next, the sections were incubated with the secondary antibodies (goat anti-rabbit IgG H&L Alexa Fluor 488 and goat anti-mouse IgG H&L Alexa Fluor 594) for 60 min at 37 °C.

Dual-staining for P-Drp and TUNEL were analyzed by immunohistochemistry. After the sections were dewaxed, repaired, blocked and sealed, the sections were incubated overnight at 4 °C with the monoclonal antibody against P-Drp1 (1:100 dilution). Next, the sections were incubated with the biotinylated secondary antibody and horseradish peroxidase-linked streptavidin for 1 h at room temperature. Peroxidase activity was demonstrated with 3,3′-Diaminobenzidine (DAB). TUNEL staining was performed using the In-Situ Cell Death Detection Kit (Roche, Mannheim, Germany).

2.9. Statistical analysis

Data were presented as mean ± standard deviation (SD) unless otherwise stated. Comparisons of the following indicators among multiple groups were made using the one-way analysis of variance (ANOVA): baseline parameters, CPR duration, apoptotic indexes, MPTPs, the overlapping coefficient of TUNEL/LC3, co-expression of P-Drp1/TUNEL, co-expression of P-Drp1/LC3 and various protein concentrations. The Kruskal-Wallis test was used for comparison of the survival rate and NDS. SPSS version 21.0 for Windows (IBM, Chicago, IL, USA) was used for the statistical analysis. Any p-values < 0.05 were considered statistically significant.

3. Results

3.1. PD98059 improved the survival and NDS of rats at 24 h post-resuscitation

As shown in Table 1, when compared to the Sham group, the CA and DMSO groups showed lower survival rates (CA, $P < 0.01$; DMSO, $P < 0.05$) and NDS (CA, DMSO, $P < 0.001$). As expected, there were no significant differences between the CA and DMSO groups. The PD-treated groups had higher survival rates than the CA group (PD0.15, $P < 0.05$; PD0.3, $P < 0.01$) and higher NDS than the CA group (PD0.15, PD0.3, $P < 0.001$) and DMSO group (PD0.3, $P < 0.001$).

Table 1
Survival rate and NDS in rats at 24 h post-resuscitation.

Group	Survival rate	n	CPR duration	NDS
Sham	15/15 (100%)	15	–	80 (80, 80)
CA	15/30 (50%)**	15	82.9 ± 15.5	68 (66, 72)***
DMSO	20/30 (66.7%)*	20	83.5 ± 11.2	69.5 (65.5, 71.5)***
PD0.15	24/30 (80%)#	24	81.2 ± 12.5	72 (69, 73)***
PD0.3	26/30 (86.7%)##	26	82.5 ± 11.3	75 (74, 76)###,$$$,@@

Survival rate is represented as a ratio, CPR duration is represented as mean ± standard deviation, NDS is represented as median ± interquartile range. CPR: cardiopulmonary resuscitation; NDS: neurological deficit scores.
* $P < 0.05$.
** $P < 0.01$.
*** $P < 0.001$ vs. the Sham group.
# $P < 0.05$.
$P < 0.01$.
$P < 0.001$ vs. the CA group.
$$$ $P < 0.001$ vs. the DMSO group.
@@ $P < 0.01$ vs. the PD0.15 group.

3.2. PD98059 decreased TUNEL positive neurons in a dose-dependent manner at 24 h post-reperfusion in the cortices of rats following CA/CPR

The fluorescence signals of TUNEL and DAPI staining in the cortex were shown in Fig. 1A. The apoptotic rates of cells were shown in Fig. 1B. The apoptotic rates in CA and DMSO groups were significantly higher than the Sham group (CA, DMSO, $P < 0.001$). The apoptosis rate in the PD0.3 group was significantly lower than the other study groups (CA, DMSO, PD0.15, $P < 0.001$).

3.3. PD98059 reduced the opening of MPTPs and the mitochondrial release of CytC in a dose-dependent manner at 24 h post-reperfusion in the cortices of rats following CA/CPR

MPTP opening activity was inversely proportional to fluorescence intensity. As shown in Fig. 2A, the fluorescence intensities in the CA and DMSO groups were significantly weaker than the Sham group (CA, DMSO, $P < 0.01$). However, the fluorescence intensity in the PD0.3 group was significantly stronger than the other study groups (CA, DMSO, PD0.15, $P < 0.05$). As shown in Fig. 2B–D, the releases of CytC from the mitochondria to the cytoplasm in CA and DMSO groups were significantly higher than the Sham group (CA, DMSO, $P < 0.05$). CytC release from the mitochondria to the cytoplasm in the PD0.3 group was significantly less than the other study groups (CA, DMSO, PD0.15, $P < 0.05$).

3.4. PD98059 significantly decreased cleaved-caspase-3 and BAX expression and increased the BCL-2 and BCL-2/BAX ratio in a dose-dependent manner at 24 h post-reperfusion in the cortices of rats following CA/CPR

As shown in Fig. 3A, there was significantly more cleaved-caspase3 generated in the CA and DMSO groups when compared with the Sham group (CA, DMSO, $P < 0.01$). Cleaved-caspase3 generation in the PD0.3 group was significantly less than the other study groups (CA, $P < 0.01$; DMSO, PD0.15, $P < 0.05$). As shown in Fig. 3B, the CA group displayed higher BAX expression than the Sham group ($P < 0.05$), while the PD0.3 group showed lower BAX expression than the other study groups (CA, DMSO, $P < 0.01$; PD0.15, $P < 0.05$).

As shown in Fig. 3C, the CA and DMSO groups displayed lower BCL-2 expression than the Sham group (CA, DMSO, $P < 0.01$). However, the PD0.3 group showed higher BCL-2 expression than the other study groups (CA, DMSO, PD0.15, P < 0.05). As shown in Fig. 3D, the BCL-2/BAX ratios in the CA and DMSO groups were lower than the Sham

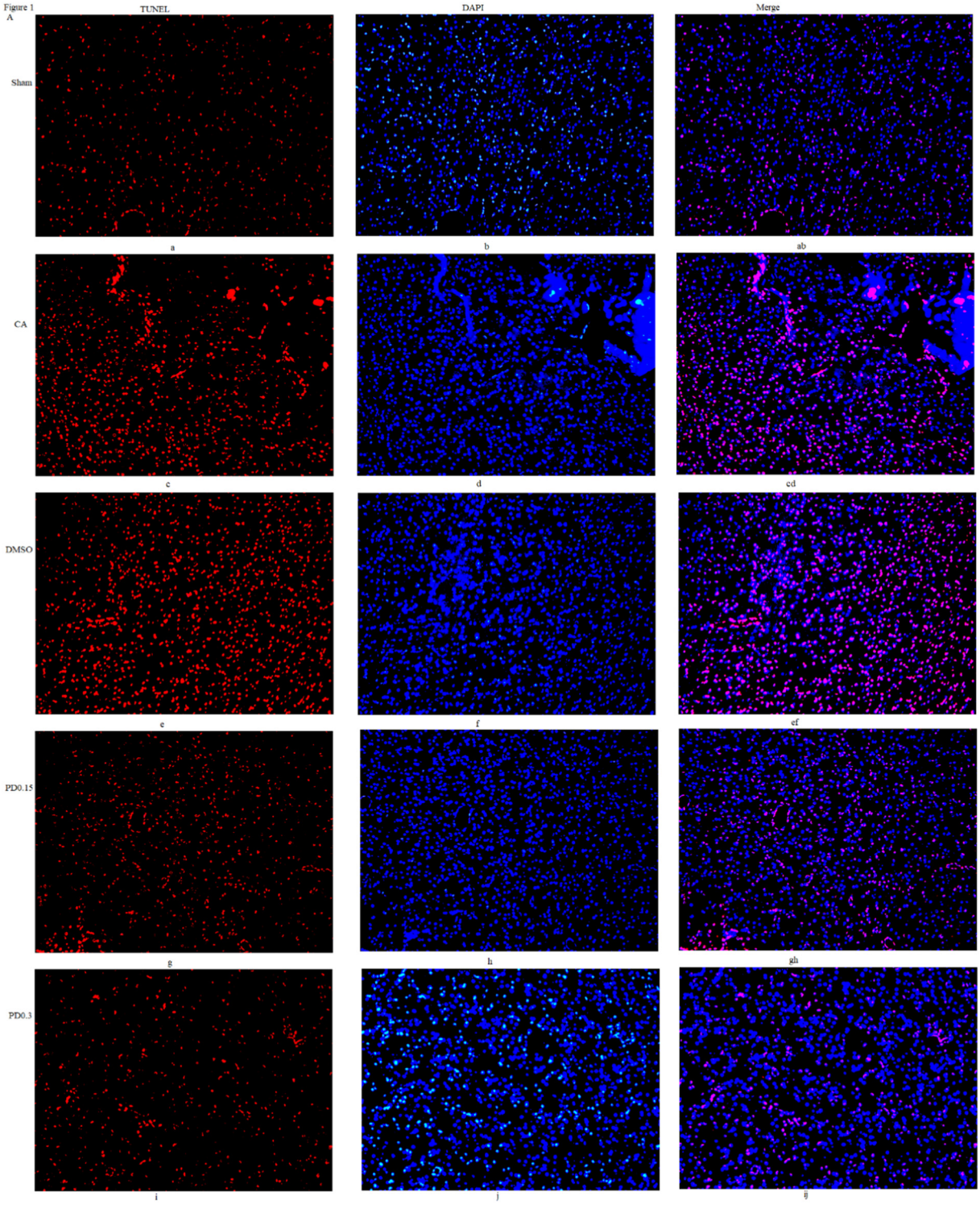

(caption on next page)

Fig. 1. Fluorescent signal of TUNEL in cortex.
A. The fluorescent signal of TUNEL and DAPI staining in cortex. TUNEL staining to monitor DNA damage (red) and DAPI staining to monitor morphological changes of nuclei (blue). (All images are shown with original magnification ×200). B. Cell apoptotic rates. All data above are represented as mean ± standard deviation. (***$P < 0.001$versus Sham group; ###P < 0.001versus CA group; @@@P < 0.001versus DMSO group; $$$P < 0.001versus PD0.15 group.)

group (CA, $P < 0.01$; DMSO, $P < 0.05$). The BCL-2/BAX ratio in the PD0.3 group was higher than the other study groups (CA, DMSO, PD0.15, $P < 0.01$).

3.5. Characterization of autophagy by TEM

The characteristic morphology of the autophagosomes and autolysosomes showed double or multi-membrane structures that contained high-electron-density substances in the CA and PD groups, whereas, more in CA group. (Fig. 4A,B) And that, every stage of autophagy feature can be detected in CA group, which were showed in Fig. 4A.

3.6. PD98059 significantly reduced LC3II and Beclin-1 expression and increased P62 expression in a dose-dependent manner at 24 h post-reperfusion in the cortices of rats following CA/CPR

As shown in Fig. 4C, LC3II/LC3I expressions in the CA and DMSO groups were significantly higher than the Sham group (CA, DMSO, $P < 0.05$). However, LC3II/LC3I expression in the PD0.3 group was significantly lower than the other study groups (CA, DMSO, PD0.15, $P < 0.05$). As shown in Fig. 4D, Beclin-1 expressions in the CA and DMSO groups were significantly higher than the Sham group (CA, DMSO, $P < 0.01$). However, Beclin-1 expression in the PD0.3 group was significantly lower than the other study groups (CA, $P < 0.01$; DMSO, PD0.15, $P < 0.05$). As shown in Fig. 4E, P62 expressions in the CA and DMSO group were significantly lower than the Sham group (CA, DMSO, $P < 0.001$). However, P62 expression in the PD0.3 group was higher than the other study groups (CA, DMSO, PD0.15 $P < 0.001$).

3.7. While PD98059 inhibited the phosphorylation of ERK1/2 (P-ERK1/2) in a dose-dependent manner at 24 h post-reperfusion in the cortices of rats following CA/CPR, the total protein levels of ERK1/2 (P-ERK1/2) remained unchanged

As shown in Fig. 5A, western blot analysis of P-ERK1/2 and ERK1/2 revealed that P-ERK1/2 was expressed significantly higher in the CA and DMSO groups when compared with the Sham group (CA, $P < 0.01$; DMSO, $P < 0.05$). P-ERK1/2 expression in the PD0.3 group was significantly lower than the other study groups (CA, $P < 0.001$; DMSO, PD0.15, $P < 0.01$). Injection of PD98059 reduced P-ERK1/2 expression in a dose-dependent manner at 24 h post-reperfusion in the rats.

3.8. PD98059 significantly decreased P-Drp1 (s616) generation in a dose-dependent manner at 24 h post-reperfusion in the cortices of rats following CA/CPR

As shown in Fig. 5B, P-Drp1 (s616) expressions in the CA and DMSO groups were significantly higher than the Sham group (CA, $P < 0.01$; DMSO, $P < 0.05$). P-Drp1 expression in the PD0.3 group was lower

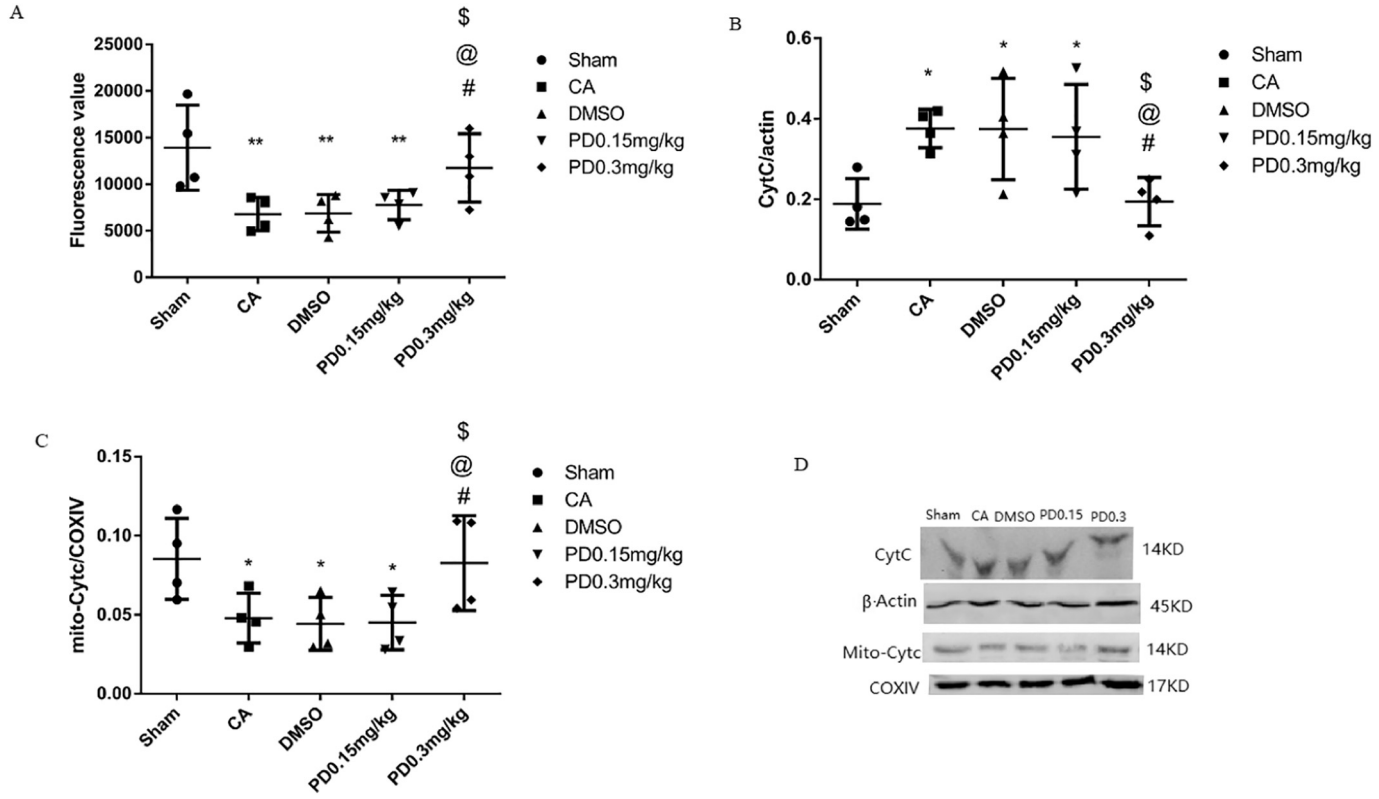

Fig. 2. Fluorescence value indicating the opening of MPTP and Western blot analysis of CytC in cytoplasm and mitochondria.
A. Fluorescence value indicating the opening of MPTP B. CytC protein in cytoplasm C. CytC protein in mitochondria D. Representative western blots of CytC in cytoplasm and mitochondria. Band intensities of CytC in cytoplasm and mitochondria were normalized to β-actin and COXIV, respectively. All data above are represented as mean ± standard deviation. $n = 4$ each group. MPTP, mitochondrial permeability transition pore (*$P < 0.05$, **$P < 0.01$versus Sham group; #P < 0.05versus CA group; @P < 0.05versus DMSO group; $P < 0.05versus PD0.15 group.)

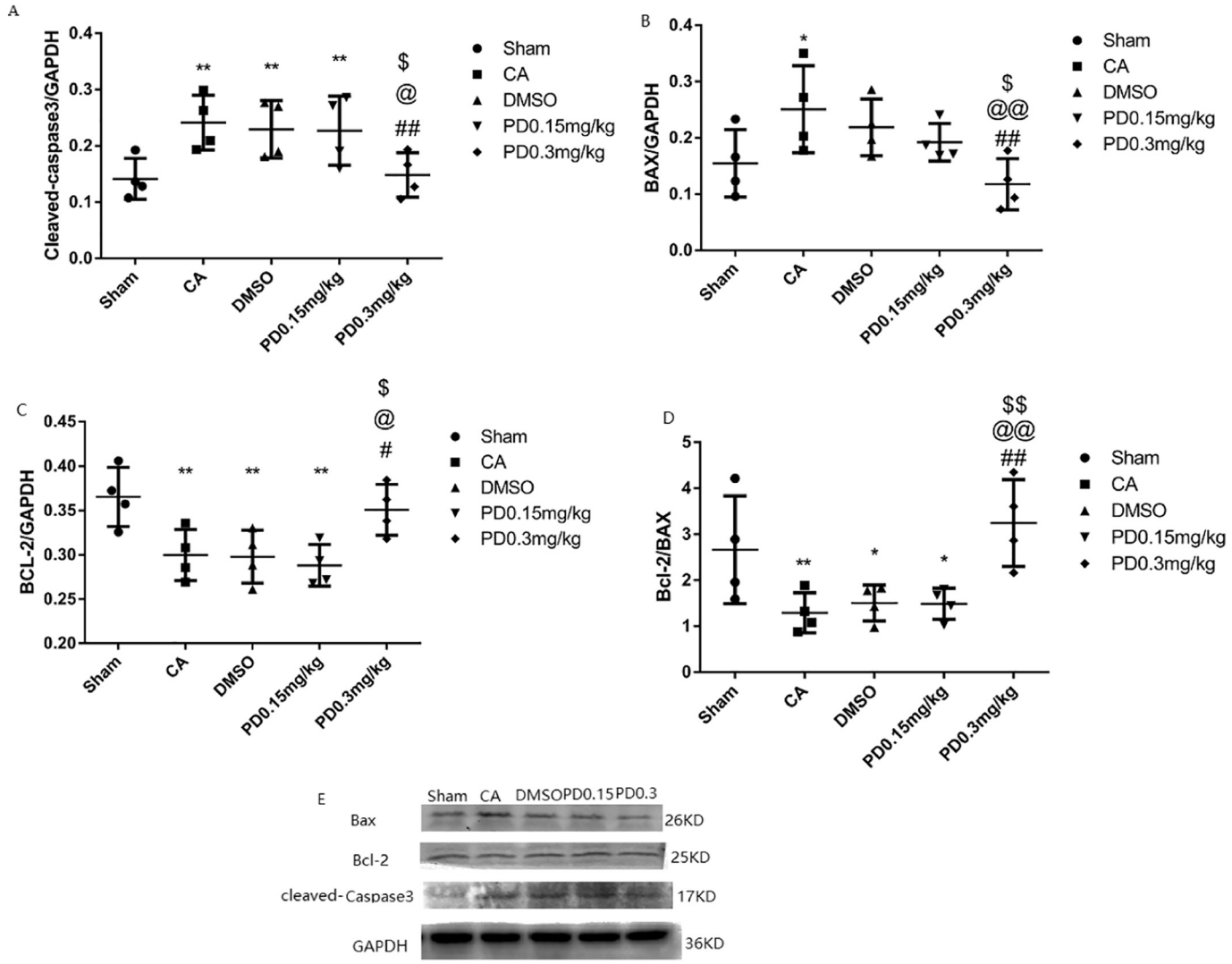

Fig. 3. Western blot analysis of cleaved-caspase3, BAX and BCL-2.
A. Western blot analysis of cleaved-caspase3 B. Western blot analysis of BAX C. Western blot analysis of BCL-2 D. The ratio of BCL-2/BAX E. Representative western blots of cleaved-caspase3, BAX and BCL-2. Band intensities were normalized to glyceraldehyde 3-phosphate dehydrogenase (GAPDH). All data above are represented as mean ± standard deviation. $n = 4$ each group. ($^{*}P < 0.05$, $^{**}P < 0.01$versus the sham group; $^{\#}P < 0.05$, $^{\#\#}P < 0.01$versus the CA group; $^{@}P < 0.05$, $^{@@}P < 0.01$versus the DMSO group; $^{\$}P < 0.05$, $^{\$\$}P < 0.01$versus the PD0.15 group.)

than the other study groups (CA, $P < 0.01$; DMSO, PD0.15, $P < 0.05$).

3.9. Dual-labeling by TUNEL and LC3, P-Drp1 and TUNEL, P-Drp1 and LC3 in the cortices of rats following CA/CPR

To corroborate the association between apoptosis and autophagy in our CA model, we examined the co-localized expression of TUNEL/LC3 by dual-stain immunofluorescence at 24 h post-reperfusion in rat cortices following CA/CPR. As shown in Fig. 6A–B, the overlapping coefficients of TUNEL/LC3 in the CA and DMSO groups were higher than the Sham group (CA, DMSO, $P < 0.001$). However, the overlap coefficient of TUNEL/LC3 in the PD0.3 group was significantly lower than the other study groups (CA, DMSO, PD0.15, $P < 0.001$).

To corroborate the association between the mitochondria dynamic protein and apoptosis in our CA model, we examined the co-localized expression of P-Drp1/TUNEL by dual-stain immunohistochemistry at 24 h post-reperfusion in rat cortices following CA/CPR. As shown in Fig. 6C–D, the co-localized expressions of P-Drp1/TUNEL in the CA and DMSO groups were higher than the Sham group (CA, DMSO, $P < 0.01$). However, the co-localized expression of P-Drp1/TUNEL in the PD0.3 group was significantly lower than the other study groups (CA, $P < 0.01$; DMSO, PD0.15, $P < 0.05$).

To corroborate the association between mitochondria dynamic protein and autophagy in our CA model, we examined the co-localized expression of P-Drp1/LC3 by dual-stain immunofluorescence at 24 h post-reperfusion in rat cortices following CA/CPR. As shown in Fig. 6E–F, the co-localized expressions of P-Drp1/LC3 in the CA and DMSO groups were higher than the Sham group (CA, DMSO, $P < 0.01$). However, the co-localized expression of P-Drp1/LC3 in the PD0.3 group was significantly lower than the other study groups (CA, DMSO, PD0.15, $P < 0.001$).

4. Discussion

In this study, we again observed PD98059-treated CPR outcomes and showed the same trend of improving the survival rate and NDS as our previous study [22].

Our study showed that PD98059 reduces apoptosis in cerebral cortical cells, which was accomplished through a mitochondrial pathway by decreasing the openings of MPTP, the release of CytC, the activation of caspase3 and increasing the expression of BCL-2. The MPTP is a large conductance channel in the mitochondrial inner

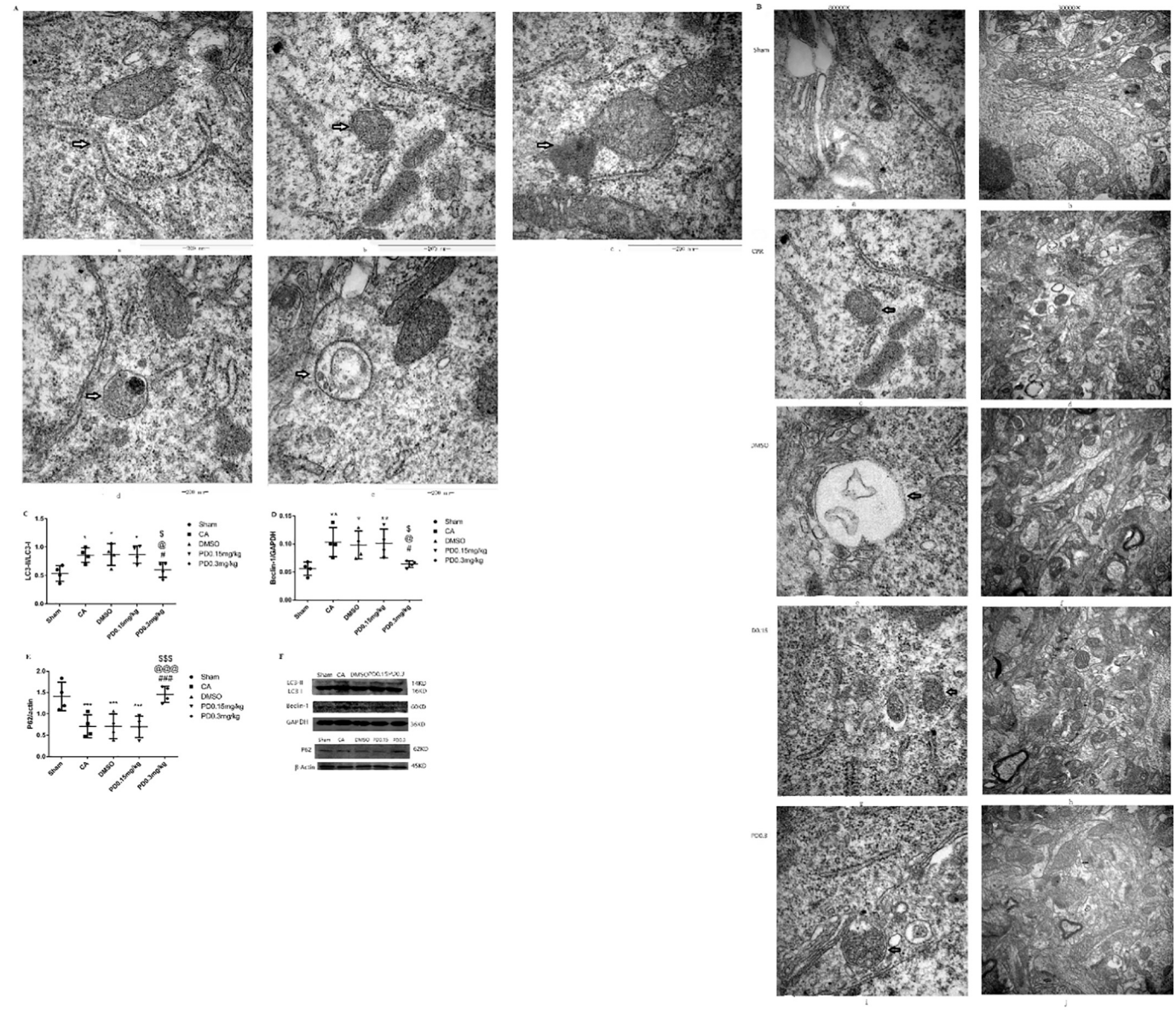

Fig. 4. Electron microscopy of autophagy and Western blot analysis of LC3, Beclin-1 and P62.
A. Every stage of autophagy feature. Autophagic bilayer membrane was indicated by arrow in a, autophagosome in b, lysosome binding with autophagosome in c, autolysosome in d, degraded autophagosome in e. Images were acquired with an electron microscope at 80000× (scale bar, 200 nm). B. Autophagy in all group. Autophagosomes and autolysosomes were indicated by arrow. Images were acquired with an electron microscope at 30000× (scale bar, 1um). A close-up from the image is shown in left panel at 80000× (scale bar, 200 nm) C. Western blot analysis of LC3II/LC3I D. Western blot analysis of Beclin-1 E. Western blot analysis of P62 F. Representative western blots of LC3II/LC3I, Beclin-1and P62. $n = 4$ each group. ($^{*}P < 0.05$, $^{**}P < 0.01$, $^{***}P < 0.001$vs Sham group; $^{\#}P < 0.05$, $^{\#\#}P < 0.01$, $^{\#\#\#}P < 0.001$vs CA group; $^{@}P < 0.05$, $^{@@@}P < 0.001$vs DMSO group; $^{\$}P < 0.05$, $^{\$\$\$}P < 0.001$vs PD0.15 group.)

membrane that allows molecules up to 1.5 kD to non-selectively pass in response to a stimulus. The irreversible opening of MPTP is involved in cell necrosis through a variety of mechanisms, including ischemia/reperfusion [26]. The opening of the MPTP leads to mitochondrial swelling and the disruption of the mitochondrial inner and outer membrane, which results in the release of CytC from the mitochondria [27] and the activation of apoptosis-related enzymes, including caspase-3 [12]. As an anti-apoptotic protein, Bcl-2 helps preserve the mitochondrial integrity by suppressing the release of CytC [28]. Previously, Li et al. [29] demonstrated that the CytC expression in the brain cytoplasm was significantly up-regulated after CPR, which resulted in the activation of apoptotic pathways. These findings are consistent with our results. ERK activity has been shown to directly lead to mitochondrial membrane disruption and CytC release in human cervical carcinoma HeLa cells and melanoma A375-S2 cells [30,31]. Our results suggest that ERK inhibition can protect the mitochondria by negatively regulating apoptosis.

Apart from apoptosis, autophagy is closely linked with CIRI. Lu et al. [19] reported that autophagy could be induced in a rat asphyxia CA/CPR model. Our study showed similar findings demonstrating increased expression of LC3-II and Beclin-1 and decreased expression of P62 at 24 h post-reperfusion in rats subjected to CA/CPR. Previous studies have shown that the activation of ERK promotes autophagy through the direct phosphorylation of Gαi3-interacting protein, a positive regulator of autophagy initiation [32]. Our work has shown that increases in autophagy activity through morphological and protein expression analyses. In terms of the morphology, every phase of autophagy was observed in the CA group, including the formation of the membrane bilayer, autophagosome formation, lysosomes binding with the autophagosomes, and the intact autolysosomes and degraded

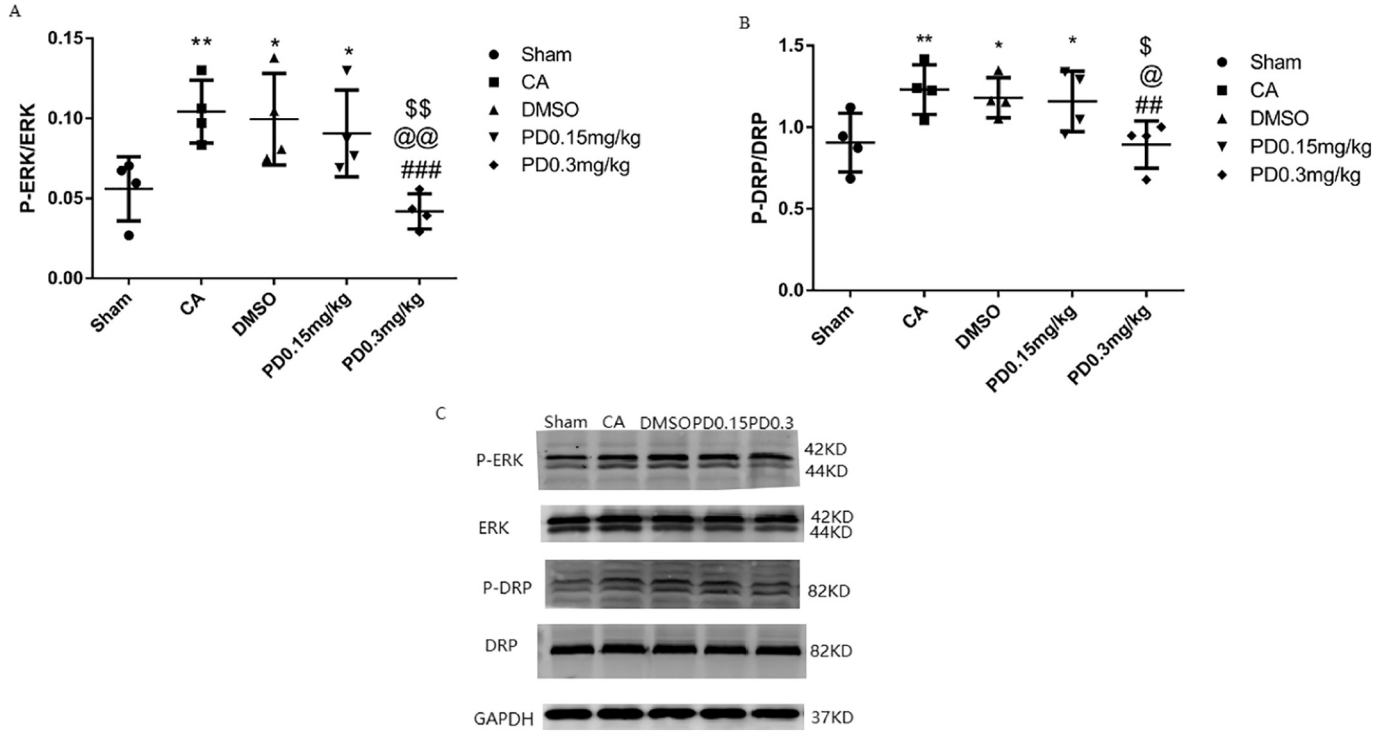

Fig. 5. Western blot analysis of P-ERK1/2, ERK1/2 and P-DRP1, DRP1.
A. Ratios of P-ERK1/2 versus ERK1/2 protein B. Ratios of P-DRP1 versus total DRP1 protein C. Representative western blots of P-ERK1/2, ERK1/2 and P-DRP1, DRP1. Band intensities normalized to GAPDH. All data above are represented as mean ± standard deviation. $n = 4$ each group. ERK, extracellular signal-regulated kinase; DRP1, dynamin related protein 1. ($^{*}P < 0.05$, $^{**}P < 0.01$ versus Sham group; $^{\#\#}P < 0.01$, $^{\#\#\#}P < 0.001$versus the CA group; $^{@}P < 0.05$, $^{@@}P < 0.01$versus DMSO group; $^{\$}P < 0.05$, $^{\$\$}P < 0.01$ versus PD0.15 group.)

autophagosomes. While a few autophagosomes were observed in the PD-treated groups, the complete processes were not observed. For the protein expression analysis, we examined the expression of Beclin-1, LC3 II and p62 to reflect activated autophagy. PD98059 reversed the increased expression of LC3-II and Beclin-1 as well as the decreased expression of P62. These results suggested that ERK inhibition helps protect the brain against excessive autophagy in CIRI. However, another researcher reported reduced levels of autophagy in a rat CA/CPR model [33]. These differences in outcomes may be due to the severity of injuries and the observational time points chosen for follow-up.

PD98059 inhibited both apoptosis and autophagy regarding with down-regulation of p-Drp1-616, which was showed by decreased double positive cells of p-Drp1/TUNET and p-Drp1/LC3 respectively in the study. Previously, ERK-mediated Drp1 phosphorylation was reported to be involved in IGF-IIR-induced autophagy [34]. In contrast, the overexpression of a Drp1-dominant negative mutant (Drp1K38A) can delay apoptosis [35]. Drp1 downregulation suppresses the formation of autophagosomes in response to glucose deprivation in cardiomyocytes [20]. Apart from Drp1, some apoptotic-related proteins can also affect autophagy. For example, the anti-apoptotic protein Bcl-2 represses autophagy by interacting with Beclin-1 [23], and dissociation of the Beclin1-Bcl-2 complex triggers autophagy. In addition, Feng et al. [36] showed that salidroside-ameliorated apoptosis and autophagy was accomplished by inhibiting the activation of MAPK signaling in a mouse ischemia reperfusion liver. In this study, increased Bcl-2 expression contributed to both apoptosis and autophagy inhibition.

In our study, the rat's rectal temperature was monitored and maintained continuously from anesthesia until rat awakening. After awakened, rats were placed in a comfortable room with constant temperature. We did not measure temperature lest disturbed resting rats. It is reported that cardiac arrest rats undergo spontaneous hypothermia that is neuroprotective strategy for post-cardiac arrest care [37]. The neuroprotective effects of spontaneous hypothermia may be adding that of PD98059, Also, similar effects offered to other groups since all rats were bred in same condition. So, the evaluation deviation for PD98059 effect is slight by grouping comparison design.

The current study has some limitations. First, there were a limited number of rats used to observe autophagy by TEM. For this reason, we were unable to provide a statistical analysis. Secondly, we did not compare the effect of PD98059 and autophagy inhibitor on cerebral autophagy at post-resuscitation. It should be further confirmed. Thirdly, we focused on mitochondrial-related mechanisms at 24 h post-reperfusion in this study and further verification of the neuroprotective mechanism of PD98059 at different time points is needed to verify our findings. Lastly, blood level of PD98059 was not measured at the end time of the experiment. The relationship between PD98059 blood concentration and its effect in 24 h and extended time after CPR still need to be probed.

In conclusion, the ERK inhibitor PD98059 alleviated apoptosis and autophagy at 24 h post-reperfusion in rats subjected to CA/CPR, indicating the potential use of ERK inhibitors for the treatment of brain injury resulting from CA in the future.

Author contributions

Conceptualization of the study: Meng-Hua Chen, Lu Xie.

Data curation: Jun-Hui Zheng, Nuo Li, Zhao-Yin Fu.

Formal analysis of the data: Jun-Hui Zheng, Tao Qin, XiaoFeng Tan, RanTao.

Funding acquisition: Meng-Hua Chen, Lu Xie, Jun-Hui Zheng.

Methodologies: Jun-Hui Zheng, Zhao-Yin Fu, XiaoFeng Tan, RanTao.

Project administration: Jun-Hui Zheng, Nuo Li, Tao Qin.

Visualization: Jun-Hui Zheng, Lu Xie, Nuo Li.

Writing the original draft: Jun-Hui Zheng, Lu Xie.

Writing, reviewing, and editing the final version: Meng-Hua Chen,

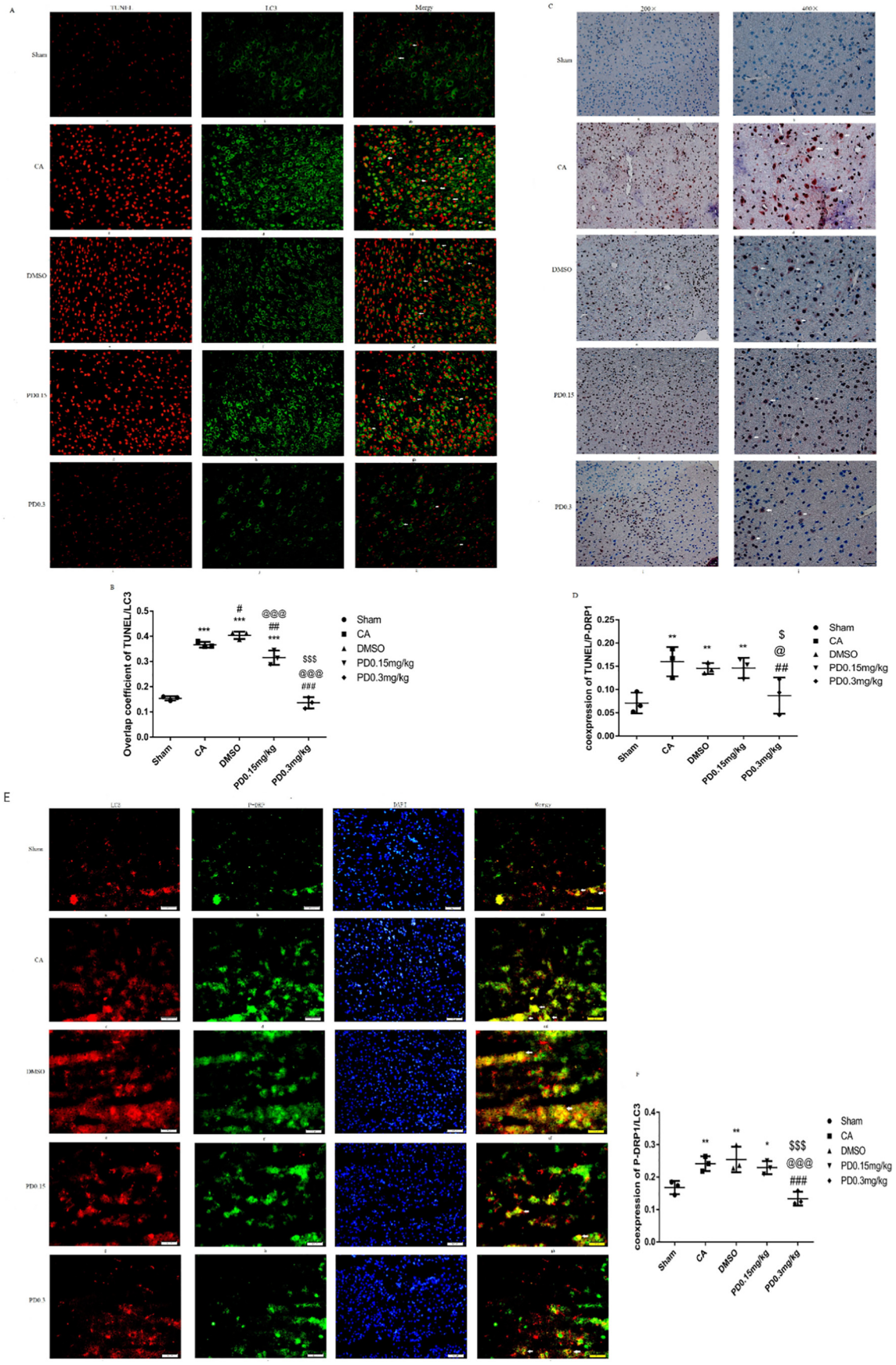

(caption on next page)

Fig. 6. Immunofluorescence double staining and immunohistochemistry double staining.
A. Immunofluorescence double staining for TUNEL and LC3 in rat cortex. TUNEL positive neurons were stained red. The cytoplasm of the cells expressing LC3 was stained green. (All images are shown with original magnification ×400). B. Overlap coefficient of TUNEL/LC3 C. Immunohistochemistry double staining for P-DRP1 and TUNEL in rat cortex. TUNEL positive neuron was stained brown. The cytoplasm of the cells expressing P-DRP1 was stained red. (a c e g i original magnification ×200, b d f h j original magnification ×400) D. Coexpressions of P-DRP1/TUNEL E. Immunofluorescence double staining for P-DRP1 and LC3 in rat cortex. The cytoplasm of the cells expressing P-Drp and LC3 was stained green and red, respectively. Co-expression of P-Drp and LC3 were stained yellow. (All images are shown with original magnification ×400) F. Coexpressions of P-DRP1/LC3 ($^{*}P < 0.05$, $^{**}P < 0.01$, $^{***}P < 0.001$ versus Sham group; $^{\#\#\#}P < 0.001$ versus CA group; $^{@}P < 0.05$, $^{@@@}P < 0.001$ versus DMSO group; $^{\$}P < 0.05$, $^{\$\$\$}P < 0.001$ versus PD0.15 group.)

Jun-Hui Zheng, Lu Xie.

Declaration of Competing Interest

No conflicts of interests to disclose.

Acknowledgments

The research was supported by the National Natural Science Foundation of China (Nos. 81160231, 81660312 and 81860333) and the Guangxi Emergency and Medical Rescue Small Highland Open Topic (No. GXJZ201414).

References

[1] C.J. Baker, A.J. Fiore, V.I. Frazzini, T.F. Choudhri, G.P. Zubay, R.A. Solomon, Intraischemic hypothermia decreases the release of glutamate in the cores of permanent focal cerebral infarcts, Neurosurgery 36 (1995) 994–1001 (discussion 1001-1002).
[2] T. Kral, H.J. Luhmann, T. Mittmann, U. Heinemann, Role of NMDA receptors and voltage-activated calcium channels in an in vitro model of cerebral ischemia, Brain Res. 612 (1993) 278–288.
[3] S. Nogawa, F. Zhang, M.E. Ross, C. Iadecola, Cyclo-oxygenase-2 gene expression in neurons contributes to ischemic brain damage, J. Neurosci. 17 (1997) 2746–2755.
[4] H. Nawashiro, K. Tasaki, C.A. Ruetzler, J.M. Hallenbeck, TNF-alpha pretreatment induces protective effects against focal cerebral ischemia in mice, J. Cereb. Blood Flow Metab. 17 (1997) 483–490.
[5] A. Hara, T. Iwai, M. Niwa, T. Uematsu, N. Yoshimi, T. Tanaka, H. Mori, Immunohistochemical detection of Bax and Bcl-2 proteins in gerbil hippocampus following transient forebrain ischemia, Brain Res. 711 (1996) 249–253.
[6] C. Horbinski, C.T. Chu, Kinase signaling cascades in the mitochondrion: a matter of life or death, Free Radic. Biol. Med. 38 (2005) 2–11.
[7] L. Galluzzi, N. Zamzami, T. de La Motte Rouge, C. Lemaire, C. Brenner, G. Kroemer, Methods for the assessment of mitochondrial membrane permeabilization in apoptosis, Apoptosis 12 (2007) 803–813.
[8] A. Dashdorj, K.R. Jyothi, S. Lim, A. Jo, M.N. Nguyen, J. Ha, K.S. Yoon, H.J. Kim, J.H. Park, M.P. Murphy, S.S. Kim, Mitochondria-targeted antioxidant MitoQ ameliorates experimental mouse colitis by suppressing NLRP3 inflammasome-mediated inflammatory cytokines, BMC Med. 11 (2013) 178.
[9] G. Ashrafi, T.L. Schwarz, The pathways of mitophagy for quality control and clearance of mitochondria, Cell Death Differ. 20 (2013) 31–42.
[10] H. Hou, Y. Wang, Q. Li, Z. Li, Y. Teng, J. Li, X. Wang, J. Chen, N. Huang, The role of RIP3 in cardiomyocyte necrosis induced by mitochondrial damage of myocardial ischemia-reperfusion, Acta Biochim. Biophys. Sin. Shanghai 50 (2018) 1131–1140.
[11] H. Zhou, S. Hu, Q. Jin, C. Shi, Y. Zhang, P. Zhu, Q. Ma, F. Tian, Y. Chen, Mff-dependent mitochondrial fission contributes to the pathogenesis of cardiac microvasculature ischemia/reperfusion injury via induction of mROS-mediated cardiolipin oxidation and HK2/VDAC1 disassociation-involved mPTP opening, J. Am. Heart Assoc. 6 (2017).
[12] M. Ott, V. Gogvadze, S. Orrenius, B. Zhivotovsky, Mitochondria, oxidative stress and cell death, Apoptosis 12 (2007) 913–922.
[13] J. Liu, X. Jiang, Q. Zhang, S. Lin, J. Zhu, Y. Zhang, J. Du, X. Hu, W. Meng, Q. Zhao, Neuroprotective effects of Kukoamine A against cerebral ischemia via antioxidant and inactivation of apoptosis pathway, Neurochem. Int. 107 (2017) 191–197.
[14] P. Li, M. Shen, F. Gao, J. Wu, J. Zhang, F. Teng, C. Zhang, An antagomir to microRNA-106b-5p ameliorates cerebral ischemia and reperfusion injury in rats via inhibiting apoptosis and oxidative stress, Mol. Neurobiol. 54 (2017) 2901–2921.
[15] X. Zhou, L. Yong, Y. Huang, S. Zhu, The Protective Effects of Distal Ischemic Treatment on Apoptosis and Mitochondrial Permeability in the Hippocampus After Cardiopulmonary Resuscitation, vol. 233, (2018), pp. 6902–6910.
[16] H. Wu, P. Wang, Y. Li, M. Wu, J. Lin, Z. Huang, Diazoxide Attenuates Postresuscitation Brain Injury in a Rat Model of Asphyxial Cardiac Arrest by Opening Mitochondrial ATP-sensitive Potassium Channels, vol. 2016, (2016), p. 1253842.
[17] Z. Su, Z. Yang, Y. Xu, Y. Chen, Q. Yu, Apoptosis, autophagy, necroptosis, and cancer metastasis, Mol. Cancer 14 (2015) 48.
[18] A.L. Edinger, C.B. Thompson, Death by design: apoptosis, necrosis and autophagy, Curr. Opin. Cell Biol. 16 (2004) 663–669.
[19] J. Lu, Y. Shen, H.Y. Qian, L.J. Liu, B.C. Zhou, Y. Xiao, J.N. Mao, G.Y. An, M.Z. Rui, T. Wang, C.L. Zhu, Effects of mild hypothermia on the ROS and expression of caspase-3 mRNA and LC3 of hippocampus nerve cells in rats after cardiopulmonary resuscitation, World J Emerg Med 5 (2014) 298–305.
[20] Y. Lee, H.Y. Lee, R.A. Hanna, A.B. Gustafsson, Mitochondrial autophagy by Bnip3 involves Drp1-mediated mitochondrial fission and recruitment of Parkin in cardiac myocytes, Am. J. Physiol. Heart Circ. Physiol. 301 (2011) H1924–H1931.
[21] E. Smirnova, D.L. Shurland, S.N. Ryazantsev, A.M. van der Bliek, A human dynamin-related protein controls the distribution of mitochondria, J. Cell Biol. 143 (1998) 351–358.
[22] P.A. Nguyen Thi, M.H. Chen, N. Li, X.J. Zhuo, L. Xie, PD98059 protects brain against cells death resulting from ROS/ERK activation in a cardiac arrest rat model, Oxidative Med. Cell. Longev. 2016 (2016) 3723762.
[23] S. Pattingre, A. Tassa, X. Qu, R. Garuti, X.H. Liang, N. Mizushima, M. Packer, M.D. Schneider, B. Levine, Bcl-2 antiapoptotic proteins inhibit Beclin 1-dependent autophagy, Cell 122 (2005) 927–939.
[24] M.H. Chen, T.W. Liu, L. Xie, F.Q. Song, T. He, Z.Y. Zeng, S.R. Mo, A simpler cardiac arrest model in rats, Am. J. Emerg. Med. 25 (2007) 623–630.
[25] X. Jia, M.A. Koenig, H.C. Shin, G. Zhen, C.A. Pardo, D.F. Hanley, N.V. Thakor, R.G. Geocadin, Improving neurological outcomes post-cardiac arrest in a rat model: immediate hypothermia and quantitative EEG monitoring, Resuscitation 76 (2008) 431–442.
[26] S.M. Davidson, D. Hausenloy, M.R. Duchen, D.M. Yellon, Signalling via the reperfusion injury signalling kinase (RISK) pathway links closure of the mitochondrial permeability transition pore to cardioprotection, Int. J. Biochem. Cell Biol. 38 (2006) 414–419.
[27] P. Dos Santos, A.J. Kowaltowski, M.N. Laclau, S. Seetharaman, P. Paucek, S. Boudina, J.B. Thambo, L. Tariosse, K.D. Garlid, Mechanisms by which opening the mitochondrial ATP- sensitive K(+) channel protects the ischemic heart, Am. J. Physiol. Heart Circ. Physiol. 283 (2002) H284–H295.
[28] J. Yang, X. Liu, K. Bhalla, C.N. Kim, A.M. Ibrado, J. Cai, T.I. Peng, D.P. Jones, X. Wang, Prevention of apoptosis by Bcl-2: release of cytochrome c from mitochondria blocked, Science 275 (1997) 1129–1132.
[29] Y. Li, P. Wang, J. Wei, R. Fan, Y. Zuo, M. Shi, H. Wu, M. Zhou, J. Lin, M. Wu, X. Fang, Z. Huang, Inhibition of Drp1 by Mdivi-1 attenuates cerebral ischemic injury via inhibition of the mitochondria-dependent apoptotic pathway after cardiac arrest, Neuroscience 311 (2015) 67–74.
[30] X. Wang, J.L. Martindale, N.J. Holbrook, Requirement for ERK activation in cisplatin-induced apoptosis, J. Biol. Chem. 275 (2000) 39435–39443.
[31] C.L. Zhang, L.J. Wu, H.J. Zuo, S. Tashiro, S. Onodera, T. Ikejima, Cytochrome c release from oridonin-treated apoptotic A375-S2 cells is dependent on p53 and extracellular signal-regulated kinase activation, J. Pharmacol. Sci. 96 (2004) 155–163.
[32] E. Ogier-Denis, S. Pattingre, J. El Benna, P. Codogno, Erk1/2-dependent phosphorylation of Galpha-interacting protein stimulates its GTPase accelerating activity and autophagy in human colon cancer cells, J. Biol. Chem. 275 (2000) 39090–39095.
[33] X. Li, Y.J. Liu, J.M. Xia, X.Y. Zeng, X.X. Liao, H.Y. Wei, C.L. Hu, X.L. Jing, G. Dai, Activation of autophagy improved the neurologic outcome after cardiopulmonary resuscitation in rats, Am. J. Emerg. Med. 34 (2016) 1511–1518.
[34] C.Y. Huang, C.H. Lai, C.H. Kuo, S.F. Chiang, P.Y. Pai, J.Y. Lin, C.F. Chang, V.P. Viswanadha, W.W. Kuo, C.Y. Huang, Inhibition of ERK-Drp1 signaling and mitochondria fragmentation alleviates IGF-IIR-induced mitochondria dysfunction during heart failure, J. Mol. Cell. Cardiol. 122 (2018) 58–68.
[35] M. Karbowski, Y.J. Lee, B. Gaume, S.Y. Jeong, S. Frank, A. Nechushtan, A. Santel, M. Fuller, C.L. Smith, R.J. Youle, Spatial and temporal association of Bax with mitochondrial fission sites, Drp1, and Mfn2 during apoptosis, J. Cell Biol. 159 (2002) 931–938.
[36] J. Feng, Q. Zhang, W. Mo, L. Wu, S. Li, J. Li, T. Liu, S. Xu, X. Fan, C. Guo, Salidroside pretreatment attenuates apoptosis and autophagy during hepatic ischemia-reperfusion injury by inhibiting the mitogen-activated protein kinase pathway in mice, Drug Des. Devel. Ther. 11 (2017) 1989–2006.
[37] R.W. Hickey, H. Ferimer, H.L. Alexander, R.H. Garman, C.W. Callaway, S. Hicks, P. Safar, S.H. Graham, P.M. Kochanek, Delayed, spontaneous hypothermia reduces neuronal damage after asphyxial cardiac arrest in rats, Crit. Care Med. 28 (2000) 3511–3516.